MicroRNA-16-5p/BIMP1/NF-κB axis regulates autophagy to exert a tumor-suppressive effect on bladder cancer

JIANI HE[1], ZHONGKAI QIU[2], HAO ZHANG[3,4], ZHIPENG GAO[3,4],
YUANJUN JIANG[3,4], ZHENHUA LI[3,4], CHUIZE KONG[3,4] and XIAOJUN MAN[3,4]

[1]Department of Breast Surgery, The First Hospital of China Medical University, Shenyang, Liaoning 110001;
[2]Department of Urology, Benxi Central Hospital, Benxi, Liaoning 117000; [3]Department of Urology,
The First Hospital of China Medical University; [4]Institute of Urology,
China Medical University, Shenyang, Liaoning 110001, P.R. China

Abstract. Bladder cancer (BC) is the second most common urological disease worldwide. Previous studies have reported that microRNA (miR)-16-5p is associated with the development of BC, but whether miR-16-5p regulates BC cell autophagy remains unknown. Thus, the aim of the present study was to investigate this issue. miR-16-5p expression in BC cells was assessed by reverse transcription-quantitative PCR. Cell viability and apoptosis were detected via Cell Counting Kit-8 and flow cytometry assays, respectively. For cell autophagy detection, autophagic flux was detected using a mCherry-green fluorescent protein-microtubule-associated proteins 1A/1B light chain 3B (LC3) puncta formation assay, followed by determination of autophagy-related protein markers. The targeting relationship between miR-16-5p and caspase recruitment domain family member 10 (BIMP1) was confirmed using a dual-luciferase reporter assay, followed by detection of the BIMP1/NF-κB signaling pathway. The results showed that miR-16-5p overexpression inhibited cell viability, whereas miR-16-5p knockdown promoted cell viability in BC. Furthermore, miR-16-5p overexpression induced autophagy, which was accompanied by increased autophagic flux and expression of the autophagy-related proteins LC3-II and beclin 1, as well as decreased p62 expression, whereas miR-16-5p silencing led to an inhibition of autophagy in BC cells. Moreover, autophagy inhibitor 3-methyladenine treatment inhibited cell autophagy and apoptosis in miR-16-5p-overexpressing cells. Mechanistic studies demonstrated that miR-16-5p could inhibit the BIMP1/NF-κB signaling pathway and this inhibition was achieved by directly targeting BIMP1. Furthermore, it was found that blockade of the BIMP1/NF-κB signaling pathway inversed the inhibitory effects of miR-16-5p knockdown on autophagy in BC cells. *In vivo* experiments further verified the tumor-suppressive effect on BC of the miR-16-5p/BIMP1/NF-κB axis. Therefore, the results of the present study indicated that miR-16-5p promotes autophagy of BC cells via the BIMP1/NF-κB signaling pathway, and an improved understanding of miR-16-5p function may provide therapeutic targets for clinical intervention in this disease.

Introduction

Bladder cancer (BC) is one of the most common malignant tumors of the urinary system and is characterized by high morbidity and mortality rates (1). A number of factors can induce BC, including smoking, environmental exposure, exposure to carcinogens and genetic factors (1,2). Surgical resection, chemotherapy and radiotherapy are the conventional treatments for BC (3). Initial tumor resection combined with adjuvant therapy increases the 5-year survival rate (4); however, BC has a high recurrence rate after surgery. It was previously demonstrated that non-muscle invasive BC has tumor recurrence and disease progression rates of up to 80 and 45%, respectively (5). Therefore, it is necessary to investigate the molecular mechanisms involved in the development of BC in order to find novel diagnostic markers and therapeutic targets.

Autophagy is a conservative self-degradation process that plays an important role in the development and treatment of cancers (6). It has been reported that the induction of autophagy inhibited breast cancer progression (7). MicroRNAs (miRs) are non-coding single-stranded RNA molecules that regulate gene expression by binding to the 3'-untranslated region (UTR) of downstream targets (8). Due to this characteristic, miRs have multiple functions, including regulating cell autophagy (9). For example, miR-16-5p, which acts as a tumor suppressor in BC, has been reported to induce autophagy of cervical carcinoma cells (10,11). It has also been observed that autophagy significantly increased in non-small cell lung carcinoma cells transfected with miR-16-5p mimics (12).

Correspondence to: Dr Xiaojun Man, Department of Urology, The First Hospital of China Medical University, 155 North Nanjing Street, Shenyang, Liaoning 110001, P.R. China
E-mail: xjman@cmu.edu.cn

These findings indicate that miR-16-5p exerts an important regulatory effect on the autophagy of cancer cells. However, whether miR-16-5p regulates autophagy in BC cells requires further investigation.

It is predicted that caspase recruitment domain family member 10 (BIMP1) may be a downstream target of miR-16-5p. BIMP1, also known as caspase recruitment domain 10, is a member of the CARMA family (13). BIMP1 has been reported to be upregulated in BC cells and BIMP1 silencing can inhibit activation of the NF-κB signaling pathway (14). The NF-κB signaling pathway is activated in numerous types of cancer, including colorectal cancer, prostate cancer and BC, and exerts a tumorigenic effect (15-17). Moreover, blocking the NF-κB signaling pathway has been found to induce autophagy (18-20). Therefore, the aim of the present study was to investigate whether the miR-16-5p/BIMP1/NF-κB axis exerts antitumor effects by regulating autophagy in BC.

Materials and methods

Cell lines. T24 and 5637 cells were purchased from Shanghai Zhong Qiao Xin Zhou Biotechnology Co., Ltd. RPMI-1640 medium (MilliporeSigma) containing 10% fetal bovine serum (Sangon Biotech Co., Ltd.) was used for cell culture in an incubator at 37°C with 5% CO_2.

Cell transfection. Cells were cultured to a density of ~90% and washed once with PBS. The supernatant was discarded and 0.25% trypsin was added to digest the cells. When the cells became round, the complete medium (RPMI-1640 medium) was added to terminate the reaction. Cells were then seeded in a 6-well plate ($2x10^5$ cells per well) and placed in an incubator at 37°C in 5% CO_2. After 24 h, the transfection experiments were performed. The 5637 cells were transfected with miR-16-5p inhibitor (50 pmol per well) or its negative control (NC; 50 pmol per well) for 24 h. T24 cells were transfected with miR-16-5p mimics (50 pmol per well) or its NC (50 pmol per well) for 24 h. The transfections were performed with 6 μl Lipofectamine® 2000 (Invitrogen; Thermo Fisher Scientific, Inc.).

After transfection for 6 h, the T24 cells were treated with the autophagy inhibitor 3-methyladenine (3-MA; 2.5 mM) for 48 h. The 5637 cells were incubated with pyrrolidine dithiocarbamate (PDTC; 20 μM) for 48 h at 37°C. For co-transfection, miR-16-5p inhibitor (50 pmol per well) and BIMP1 small interfering (si)RNA (50 pmol per well) or its NC (50 pmol per well) was co-transfected into 5637 cells for 24 h with Lipofectamine 2000, according to the manufacturer's instructions. All of the transfections were performed at room temperature. All cells were transfected and dosed up for the appropriate duration, and follow-up experiments were conducted immediately. The BIMP1 and NC siRNA, miR-16-5p mimics, mimics NC and miR-16-5p inhibitor and inhibitor NC were purchased from JTS Scientific Ltd. The sequences used for the present study are presented in Table I.

Reverse transcription-quantitative PCR (RT-qPCR). Total RNA was extracted from BC cells with TriPure Isolation Reagent (BioTeke Corporation) and the concentration was determined using a NanoDrop 2000 UV spectrophotometer

(Thermo Fisher Scientific, Inc.). Next, cDNA was obtained via reverse transcription using Super M-MLV Reverse Transcriptase (BioTeke Corporation), dNTPs (Beijing Solarbio Science & Technology Co., Ltd.) and RNase inhibitor (BioTeke Corporation). Finally, using the cDNA template, primers, SYBR Green (Millipore Sigma) and 2X Power Taq PCR MasterMix (BioTeke Corporation), qPCR was performed and the relative mRNA expression level was calculated using the $2^{-\Delta\Delta Cq}$ method (21). The thermocycling conditions for qPCR were as follows: For miRNA, 94°C for 4 min, followed by 40 cycles of 94°C for 15 sec, 60°C for 20 sec and 72°C for 15 sec; and for mRNA, 94°C for 5 min, followed by 40 cycles of 94°C for 15 sec, 60°C for 25 sec and 72°C for 30 sec. miRNA and mRNA expression levels were normalized to ribosomal 5S RNA and β-actin, respectively. The primers used for qPCR are presented in Table II.

Cell proliferation assay. BC cell viability was analyzed via Cell Counting Kit-8 (CCK-8) assay (Beyotime Institute of Biotechnology). Briefly, cells were seeded in a 96-well plate at a density of $4x10^3$ per well. After transfection and treatments, the supernatant was discarded and complete medium (100 μl) was added to each well. Then, 10 μl CCK-8 was added to each well and cells were incubated at 37°C for 1 h. Finally, the optical density (OD) value at 450 nm was calculated using a microplate reader (BioTek Instruments, Inc.).

Cell apoptosis assay. Cell apoptosis was detected by flow cytometry. Briefly, after transfection and treatments, cells were washed once with PBS and then centrifuged (300 x g) for 5 min at room temperature and the supernatant was discarded. After washing twice with PBS, cells were stained with Annexin V-FITC (5 μl) and propidium iodide (5 μl). After incubation at room temperature in the dark for 15 min, the apoptosis rate was detected by flow cytometry (NovoCyte; ACEA Bioscience, Inc.) and analyzed by NovoExpress (version 1.2.5; ACEA Biosciences, Inc.).

Western blotting. Total proteins were extracted using Western and IP cell lysate (cat. no. P0013; Beyotime Institute of Biotechnology) mixed with PMSF (cat. no. ST506; Beyotime Institute of Biotechnology) and the total protein concentration was determined using a BCA protein assay kit (Beyotime Institute of Biotechnology) according to the manufacturer's instructions. Proteins were separated via SDS-PAGE (20-40 μg/lane; 8, 10 and 14%). After electrophoresis, the separated proteins were transferred onto the PVDF membranes and blocked with 5% skimmed milk for 1 h at room temperature. The membranes were subsequently incubated with primary antibodies overnight at 4°C, followed by incubation with horseradish peroxidase (HRP)-conjugated secondary antibodies for 45 min at 37°C. Finally, the proteins were visualized with ECL chemiluminescent reagent (Beyotime Institute of Biotechnology) and the OD of the target proteins was analyzed using a gel image processing system (Gel-Pro-Analyzer 4.0; Media Cybernetics, Inc.). The following primary antibodies (1:1,000) used for western blotting were purchased from ABclonal Biotech Co., Ltd.: Microtubule-associated proteins 1A/1B light chain 3B (LC3; cat. no. A19665), beclin 1 (cat. no. A7353),

Table I. Sequences used for transfection.

Sequence type	Sequence (5'-3')
BIMP1 siRNA	Forward: GGAUGAGAACUACAUGAUCTT
	Reverse: GAUCAUGUAGUUCUCAUCCTT
siRNA NC	Forward: UUCUCCGAACGUGUCACGUTT
	Reverse: ACGUGACACGUUCGGAGAATT
miR-16-5p mimics	Forward: UAGCAGCACGUAAAUAUUGGCG
	Reverse: CCAAUAUUUACGUGCUGCUAUU
Mimics NC	Forward: UUCUCCGAACGUGUCACGUTT
	Reverse: ACGUGACACGUUCGGAGAATT
miR-16-5p inhibitor	CGCCAAUAUUUACGUGCUGCUA
Inhibitor NC	UUGUACUACACAAAGUACUG

si, small interfering; NC, negative control; miR, microRNA.

Table II. Primers used for qPCR.

	Primers (5'-3')	
Gene	Forward	Reverse
miR-16-5p	TAGCAGCACGTAAATATTGGCG	GCAGGGTCCGAGGTATTC
5S rRNA	GATCTCGGAAGCTAAGCAGG	TGGTGCAGGGTCCGAGGTAT
BIMP1	GGTGCCGAGCCCTTCTACATT	TCCAGGTCCCGCAGAGTGAG
β-actin	CTTAGTTGCGTTACACCCTTTCTTG	CTGTCACCTTCACCGTTCCAGTTT

miR, microRNA; 5S rRNA, ribosomal 5S RNA.

p62 (cat. no. A19700), IκBα (cat. no. A1187), p-IκBα (ser32; cat. no. AP0707), NF-κB (cat. no. A19653) and BIMP1 (cat. no. A7368). Histone H3 primary antibody (1:2,000) was purchased from Abgent Biotech Co., Ltd. (cat. no. AM8433) and β-actin primary antibody (1:1,000) was obtained from Santa Cruz Biotechnology, Inc. (cat. no. sc-47778). The following secondary antibodies (1:5,000) were purchased from Beyotime Institute of Biotechnology: Goat anti-rabbit IgG (cat. no. A0208) and goat anti-mouse IgG (cat. no. A0216).

mCherry-green fluorescent protein (GFP)-LC3 puncta formation assay. Cells were seeded in 6-well plates at a density of $2x10^5$ cells per well. The mCherry-GFP-LC3 plasmids (1 μg per well) and miR-16-5p mimics, miR-16-5p inhibitor or its NC were co-transfected into BC cells for 48 h at room temperature. The co-transfection was performed with Lipofectamine 2000. Finally, the puncta were observed under a fluorescence microscope (magnification, x400; Olympus Corporation). Yellow and red dots represent autophagosomes and autolysosomes, respectively.

Electrophoretic mobility shift assay. Nuclear proteins were extracted from BC cells using the Nuclear Protein Extraction kit (Beyotime Institute of Biotechnology). The protein lysate was obtained as previously described for western blotting. Following centrifugation, cytoplasmic protein extraction reagent (200 μl/20 μl cell pellet; Beyotime

Institute of Biotechnology) containing PMSF was added to the pellet. The cell pellet was vigorously vortexed on the highest setting for 5 sec and incubated on ice for 10-15 min. Subsequently, cytoplasmic protein extraction reagent (10 μl; Beyotime Institute of Biotechnology) was added and vortexed for 5 sec on the highest setting and centrifuged for 5 min (4°C) at 12,000 x g. The pellet was collected again and treated with nuclear protein extraction reagent (50 μl; Beyotime Institute of Biotechnology) containing PMSF. The tubes containing the pellet were vortexed on the highest setting for 15-30 sec, every 1-2 min for a total duration of 30 min. Following centrifugation for 5 min (4°C) at 12,000 x g, the supernatant was obtained, which only contained nuclear protein. The concentration was detected using a BCA Protein assay kit (Beyotime Institute of Biotechnology). After nuclear proteins were incubated with the biotin-labeled probe for 20 min at room temperature, electrophoresis was performed using 6.5% polyacrylamide gels. After separation on polyacrylamide gels, nuclear proteins were transferred onto nylon membranes and the membranes were cross-linked under UV light for 30 min. After incubation in the streptavidin-HRP (Viagene Biotech) reaction solution for 20 min at room temperature, the membranes were visualized with the ECL chemiluminescent reagent. Finally, the OD value was calculated.

Dual-luciferase reporter assay. The binding sites between miR-16-5p and BIMP1 were determined using

TargetScanHuman (version 7.2; http://www.targetscan.org/vert_72/). miR-16-5p was searched and multiple genes that miR-16-5p may target were obtained. UTRs between BIMP1 and miR-16-5p were also searched to obtain the target binding sequence between miR-16-5p and BIMP1. The luciferase reporter assay was performed using T24 cells. Briefly, T24 cells were co-transfected with mutant (MUT) or wild-type (WT) plasmid (1.25 μg per well) containing the 3'-UTR of BIMP1 and miR-16-5p mimics (15 pmol per well) or its NC (15 pmol per well), respectively. After 48 h, the cells were harvested and luciferase activity was detected using a Luciferase Detection kit (Promega Corporation) according to the manufacturer's protocols. Relative luciferase activities were evaluated through the ratio of firefly luciferase to *Renilla* luciferase.

Xenograft tumor model. The present study was approved by The China Medical University Laboratory Animal Welfare and Ethical Committee (approval no. KT2020037) and animal experiments were performed in accordance with the Guidelines for the Care and Use of Laboratory Animals (22). Twelve male BALB/c nude mice (age, 6 weeks old; weight, 18±2 g) were purchased from Huafukang Biotechnology Co., Ltd. and housed under the following conditions: 12 h light/dark cycle, 45-55% humidity and a temperature of 24±1°C. All mice had free access to food and water. The mice (n=12) were randomly divided into the following two groups: i) Mimics NC group (n=6), mice were injected subcutaneously (right armpit) with T24 cells (1x10^7) transfected with mimics NC; and ii) miR-16-5p mimics group (n=6), mice were injected subcutaneously with T24 cells (1x10^7) transfected with miR-16-5p mimics. The tumor volume was measured every 3 days from day 6. The maximum xenograft tumor size was 334.75 mm^3. On day 24, mice were euthanized by an intraperitoneal injection of sodium pentobarbital (150 mg/kg), the tumor weight was recorded and tumor tissue samples were preserved in 4% paraformaldehyde in an ultra-low temperature refrigerator at -70°C for subsequent experiments.

Immunofluorescence staining. Tumor tissue samples were fixed using 4% paraformaldehyde for 48 h at room temperature, embedded in paraffin and cut into 5-μm sections. The sections were first blocked with normal goat serum (stock solution, Beijing Solarbio Science & Technology Co., Ltd.) for 15 min at room temperature. The tumor sections were treated with the primary antibody, LC3 obtained from Santa Cruz Biotechnology, Inc. (1:50; cat. no. sc-376404) at 4°C overnight and then incubated with the secondary antibody Cy3-labeled goat anti-mouse IgG obtained from Beyotime Institute of Biotechnology (1:200; cat. no. A0521) at room temperature for 1 h. Following DAPI staining, the cover slips were mounted and visualized using a fluorescence microscope (magnification, x400; Olympus Corporation).

Statistical analysis. An unpaired t-test was used to compare the differences between two groups. Differences among ≥3 groups were analyzed by one-way ANOVA with Tukey's multiple comparisons test. Data are expressed as the means ± SD. Data analysis was performed using GraphPad Prism 8.0 (GraphPad Software, Inc.) and P<0.05 was considered to indicate a statistically significant difference.

Results

miR-16-5p promotes autophagy in BC cells. In order to investigate the role of miR-16-5p in the autophagy of BC cells, the expression of miR-16-5p in 5637 and T24 cells was determined. It was found that the expression of miR-16-5p in T24 cells was lower than that in 5637 cells (Fig. 1A). miR-16-5p was overexpressed in T24 cells via transfection with miR-16-5p mimics, whereas miR-16-5p expression was knocked down in 5637 cells via transfection with miR-16-5p inhibitor (Fig. 1B). As presented in Fig. 1C, miR-16-5p overexpression significantly decreased the viability of BC cells, whereas miR-16-5p knockdown significantly increased cell viability when compared with the corresponding control group. As shown in Fig. 1D, miR-16-5p overexpression led to an increase in free yellow puncta and red puncta (indicating autolysosomes) and the merged colors were more towards red, indicating that miR-16-5p overexpression increased the formation of autophagosomes and autolysosomes, and that autophagic flux was promoted. However, no apparent yellow or red spots were observed in the miR-16-5p inhibitor group (Fig. 1D). Furthermore, the expression levels of autophagy-related proteins were detected via western blotting. The results demonstrated that the LC3-II/I ratio and beclin 1 protein levels in the miR-16-5p mimics group were significantly higher than those in the mimics NC group, whereas miR-16-5p knockdown notably decreased their levels as compared with the inhibitor NC (Fig. 1E). By contrast, the protein expression of p62 was notably decreased by miR-16-5p mimics, whereas its expression was significantly increased by transfection with miR-16-5p inhibitor as compared with the corresponding control group (Fig. 1E). Therefore, these results indicated that miR-16-5p induced autophagy and this may be achieved by increasing autophagic flux and the formation of autophagosomes in BC cells.

Inhibition of autophagy attenuates the promoting effect of miR-16-5p overexpression on apoptosis of BC cells. Subsequently, whether there is an association between autophagy and apoptosis in BC was investigated. As presented in Fig. 2A, miR-16-5p overexpression significantly decreased cell viability, whereas 3-MA treatment increased cell viability as compared with the miR-16-5p mimics group. Furthermore, miR-16-5p overexpression significantly increased LC3-II/I ratio and beclin 1 protein expression levels, whereas it decreased p62 expression, which was reversed by treatment with 3-MA (Fig. 2B). Notably, 3-MA treatment also decreased miR-16-5p overexpression-induced apoptosis in BC cells (Fig. 2C). Overall, these results suggested that autophagy and apoptosis are interrelated in the progression of BC. Specifically, the inhibition of autophagy could weaken the promoting effect of miR-16-5p overexpression on apoptosis.

miR-16-5p overexpression inhibits the BIMP1/NF-κB signaling pathway by directly targeting BIMP1 in BC cells. According to the prediction of TargetScanHuman, miR-16-5p may have binding sites with BIMP1 (Fig. 3A). In addition, the targeting relationship between miR-16-5p and BIMP1 was verified using a dual-luciferase reporter assay. The results showed
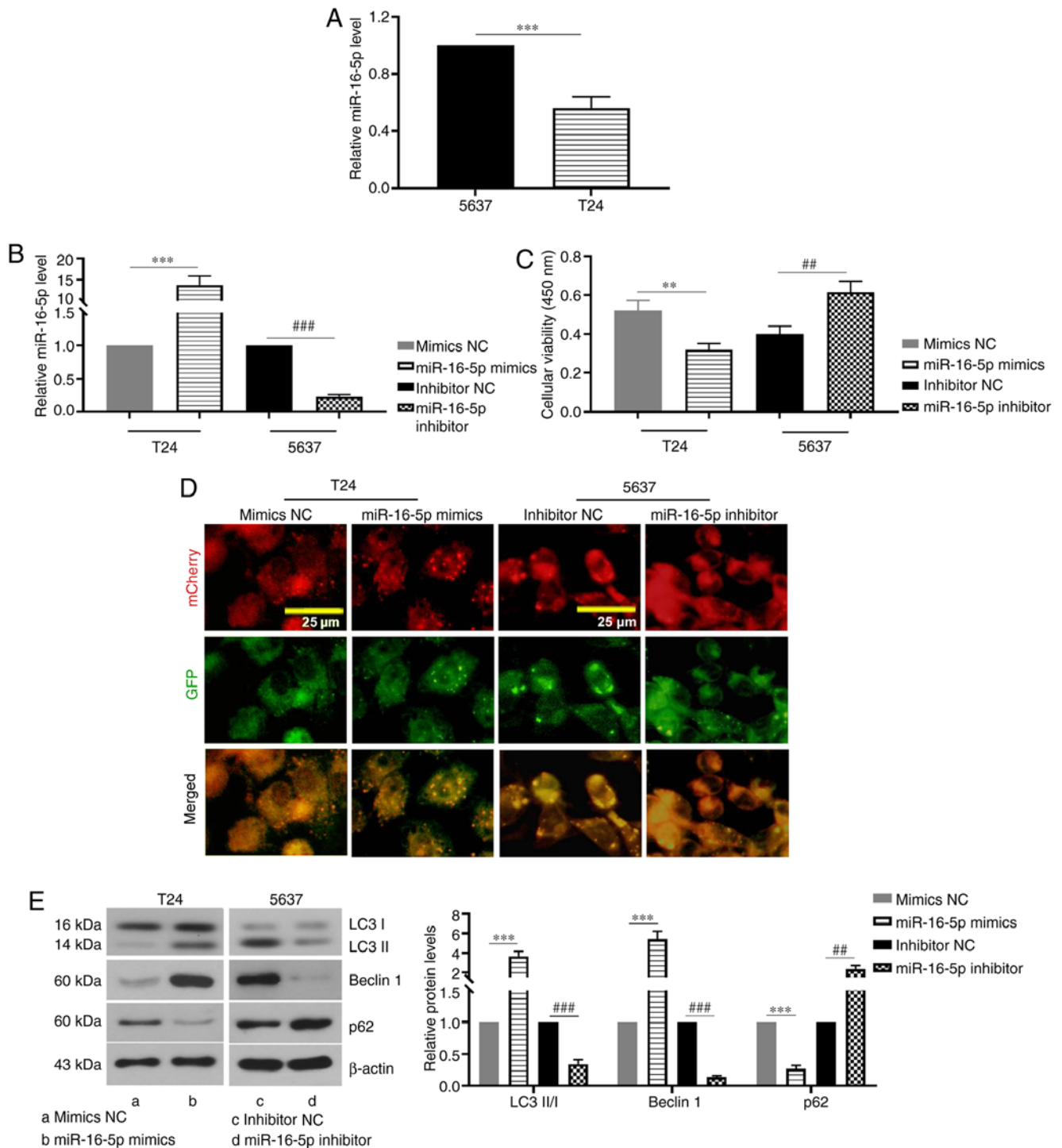
Figure 1. miR-16-5p promotes autophagy in bladder cancer cells. (A) Relative miR-16-5p expression levels in 5637 and T24 cells. (B) Relative miR-16-5p expression levels after 5637 and T24 cells were transfected with miR-16-5p mimics, inhibitor or the NC. (C) Viability of 5637 and T24 cells after transfection with miR-16-5p mimics, inhibitor or the NC. (D) Representative fluorescence images of autophagosomes and autolysosomes in 5637 and T24 cells after co-transfection with mCherry-GFP-LC3 plasmid and miR-16-5p mimics, inhibitor or the NC (magnification, x400). (E) Relative LC3-II/I, beclin 1 and p62 protein expression levels in 5637 and T24 cells transfected with miR-16-5p mimics, inhibitor or the NC (n=3). Data are presented as the means ± SD. **$P<0.01$, ***$P<0.001$, ##$P<0.01$, ###$P<0.001$. miR, microRNA; NC, negative control; GFP, green fluorescent protein; LC3, microtubule-associated proteins 1A/1B light chain 3B.

that the luciferase activity in the WT-BIMP1 + miR-16-5p mimics group was significantly lower than that of the other three groups (Fig. 3A). In addition, the mRNA and protein expression levels of BIMP1 were significantly reduced by miR-16-5p mimics, whereas miR-16-5p knockdown increased BIMP1 expression (Fig. 3B and C). Furthermore, the overexpression of miR-16-5p increased the protein expression of IκBα

and decreased the expression of phosphorylated (p)-IκBα. However, miR-16-5p knockdown decreased IκBα protein expression and increased the expression of p-IκBα (Fig. 3D). When miR-16-5p was overexpressed, NF-κB protein expression in the cytoplasm was significantly increased, whereas NF-κB protein expression in the cell nucleus and NF-κB activity was decreased (Fig. 3D and E). However, miR-16-5p
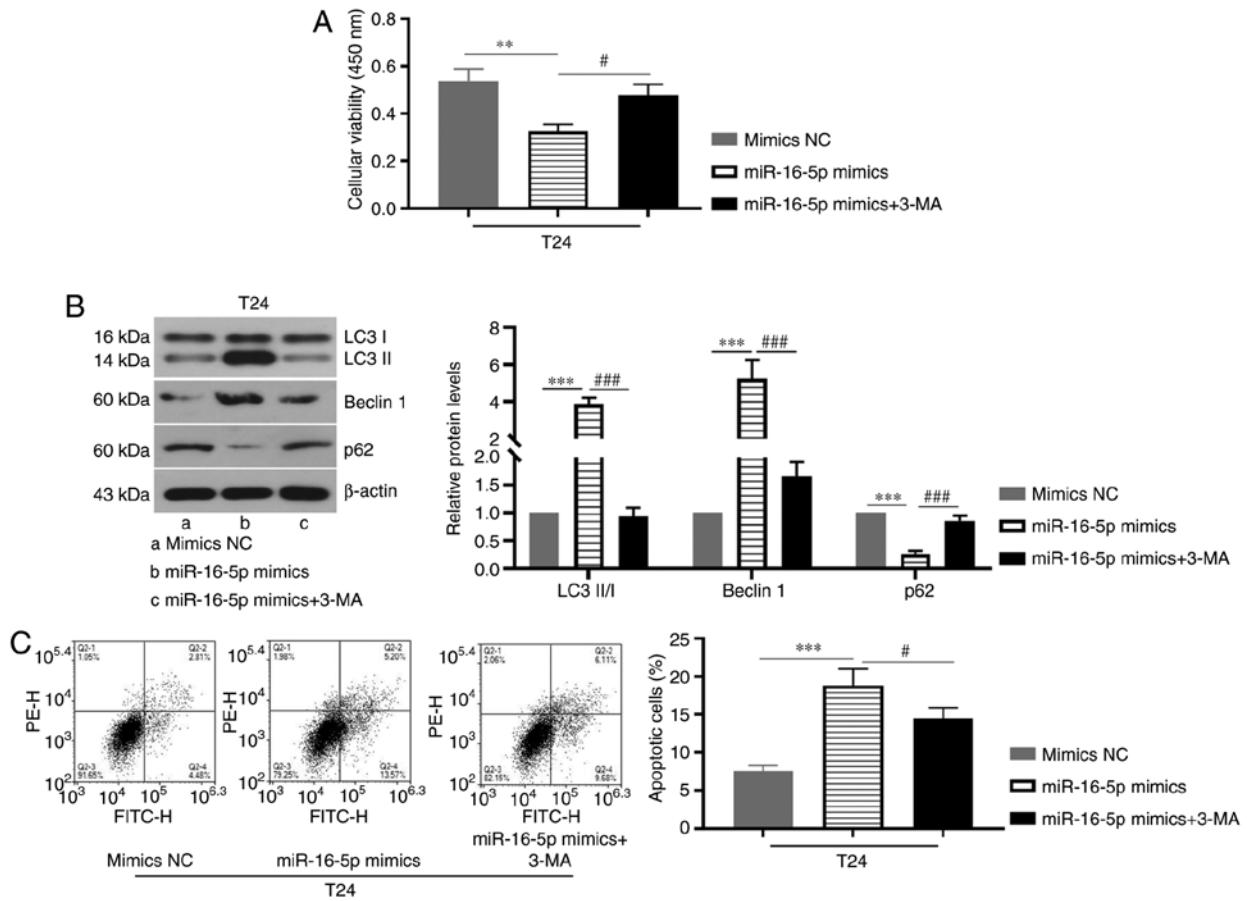
Figure 2. Inhibition of autophagy attenuates the promoting effect of miR-16-5p overexpression on the apoptosis of bladder cancer cells. (A) Viability of T24 cells after transfection with miR-16-5p mimics or NC followed by 3-MA treatment. (B) Relative LC3-II/I, beclin 1 and p62 protein expression levels in T24 cells after transfection with miR-16-5p mimics or NC followed by 3-MA treatment. (C) Apoptotic rate of T24 cells after transfection with miR-16-5p mimics or its NC followed by 3-MA treatment (n=3). Data are presented as the means ± SD. **P<0.01, ***P<0.001, #P<0.05, ###P<0.001. miR, microRNA; NC, negative control; 3-MA, 3-methyladenine; LC3, microtubule-associated proteins 1A/1B light chain 3B.

knockdown had the opposite effects on the protein expression and activity of NF-κB (Fig. 3D and E). Taken together, the results indicated that miR-16-5p negatively regulated the BIMP1/NF-κB signaling pathway via binding to BIMP1 in BC cells.

miR-16-5p promotes autophagy by blocking the BIMP1/NF-κB signaling pathway in BC cells. After transfection with the miR-16-5p inhibitor, 5,637 cells were treated with small interfering (si)-BIMP1, the NC or the NF-κB pathway inhibitor PDTC to investigate whether miR-16-5p regulates autophagy in BC cells via the BIMP1/NF-κB signaling pathway. The BIMP1 knockdown efficiency in 5637 cells was first verified. The results showed that BIMP1 siRNA transfection significantly decreased the BIMP1 protein level (Fig. 4A). As presented in Fig. 4B, miR-16-5p knockdown significantly increased cell viability, whereas BIMP1 knockdown or PDTC treatment reversed this effect. Furthermore, PDTC treatment increased the LC3-II/I ratio and the protein expression levels of and beclin 1, but decreased p62 expression when compared with the miR-16-5p inhibitor group (Fig. 4C). Similarly, BIMP1 knockdown also increased the LC3-II/I ratio and beclin 1 protein expression levels and decreased p62 expression when compared with the miR-16-5p inhibitor + si-NC group (Fig. 4C). Thus, the results suggested that inhibition of

the BIMP1/NF-κB signaling pathway reversed the inhibitory effects of miR-16-5p knockdown on autophagy in BC cells.

miR-16-5p overexpression suppresses tumor growth in mice. T24 cells transfected with mimics NC or miR-16-5p mimics were injected subcutaneously into the nude mice. The expression of miR-16-5p was analyzed via RT-qPCR, which demonstrated that the injection of cells transfected with miR-16-5p mimics significantly increased miR-16-5p expression in tumor tissues (Fig. 5A). Tumor growth was detected every 3 days. The results showed that miR-16-5p overexpression decreased tumor volume and weight (Fig. 5B-D). The results of immunofluorescence staining showed that LC3 expression in the tumor tissue samples was significantly increased by miR-16-5p overexpression (Fig. 5E). In addition, miR-16-5p overexpression increased the protein expression level of p65 in the cytoplasm and the LC3-II/I ratio, whereas it decreased the protein expression levels of BIMP1 and p65 protein in nucleus (Fig. 5F). Taken together, these data indicated that miR-16-5p overexpression inhibited tumor growth.

Discussion

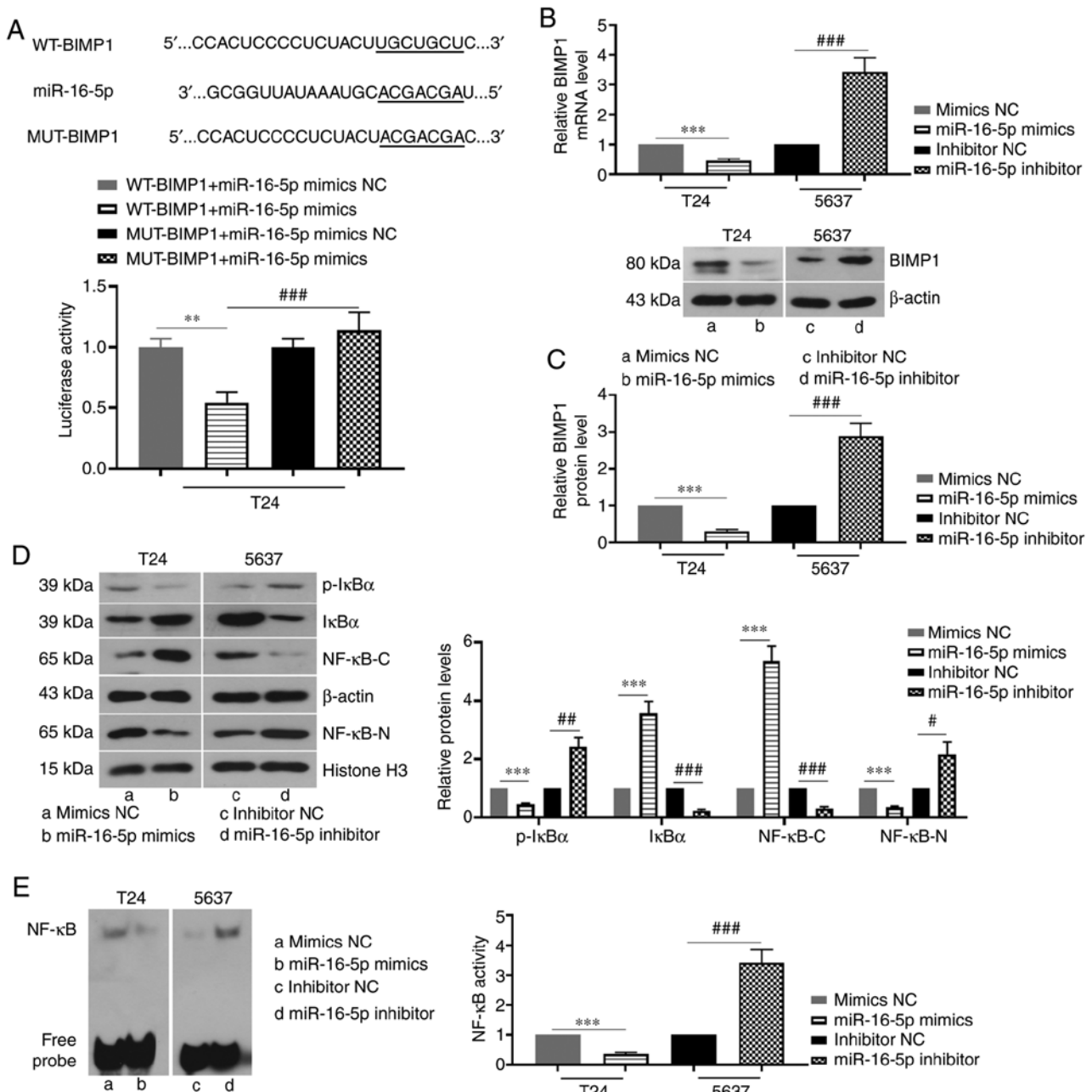The present study elucidated the regulatory mechanisms of miR-16-5p and the BIMP1/NF-κB signaling pathway in the

Figure 3. miR-16-5p overexpression inhibits the BIMP1/NF-κB signaling pathway by directly targeting BIMP1 in bladder cancer cells. (A) Binding sites of miR-16-5p to the 3'-untranslated region of BIMP1 as predicted by TargetScanHuman 7.2, and the targeting relationship between them was verified by a dual-luciferase reporter assay in T24 cells. (B and C) Relative mRNA and protein expression levels of BIMP1 in 5637 and T24 cells following transfection with miR-16-5p mimics, inhibitor or the NC. (D) Relative protein expression levels of IκBα/p-IκBα (ser32) and NF-κB in the cytoplasm (NF-κB-C) and nucleus (NF-κB-N) following transfection with miR-16-5p mimics, inhibitor or the NC. (E) NF-κB activity in 5637 and T24 cells after transfection with miR-16-5p mimics, inhibitor or the NC, as detected by electrophoretic mobility shift assay (n=3). Data are presented as the means ± SD. **P<0.01, ***P<0.001, #P<0.05, ##P<0.01, ###P<0.001. miR, microRNA; NC, negative control; p-, phosphorylated; WT, wild-type; MUT, mutant; BIMP1, caspase recruitment domain family member 10.

autophagy of BC cells. It was found that miR-16-5p induced BC cell autophagy and further promoted apoptosis. miR-16-5p negatively regulated the BIMP1/NF-κB signaling pathway by directly targeting BIMP1. The induction of autophagy by miR-16-5p overexpression was mediated through the BIMP1/NF-κB signaling pathway. These findings provided novel insight into the molecular mechanism underlying BC cell autophagy and indicated that miR-16-5p may be a target for the treatment of BC.

With increasing numbers of studies into miRs, various miRs have been found to be dysregulated during cancer development,

and they have been demonstrated to be involved in cancer cell proliferation, apoptosis and autophagy, which suggests that miRs may represent potential targets for cancer diagnosis and treatment (23). It has been reported that miR-16-5p was down-regulated in BC tissues and cells, and miR-16-5p silencing led to a decrease in BC cell viability (11,24), which was consistent with the findings of the present study.

In addition, overexpression of miR-16-5p induces autophagy in non-small cell lung carcinoma cells (12). Autophagy is a highly conserved process of self-degradation. By preventing the accumulation of damaged proteins and
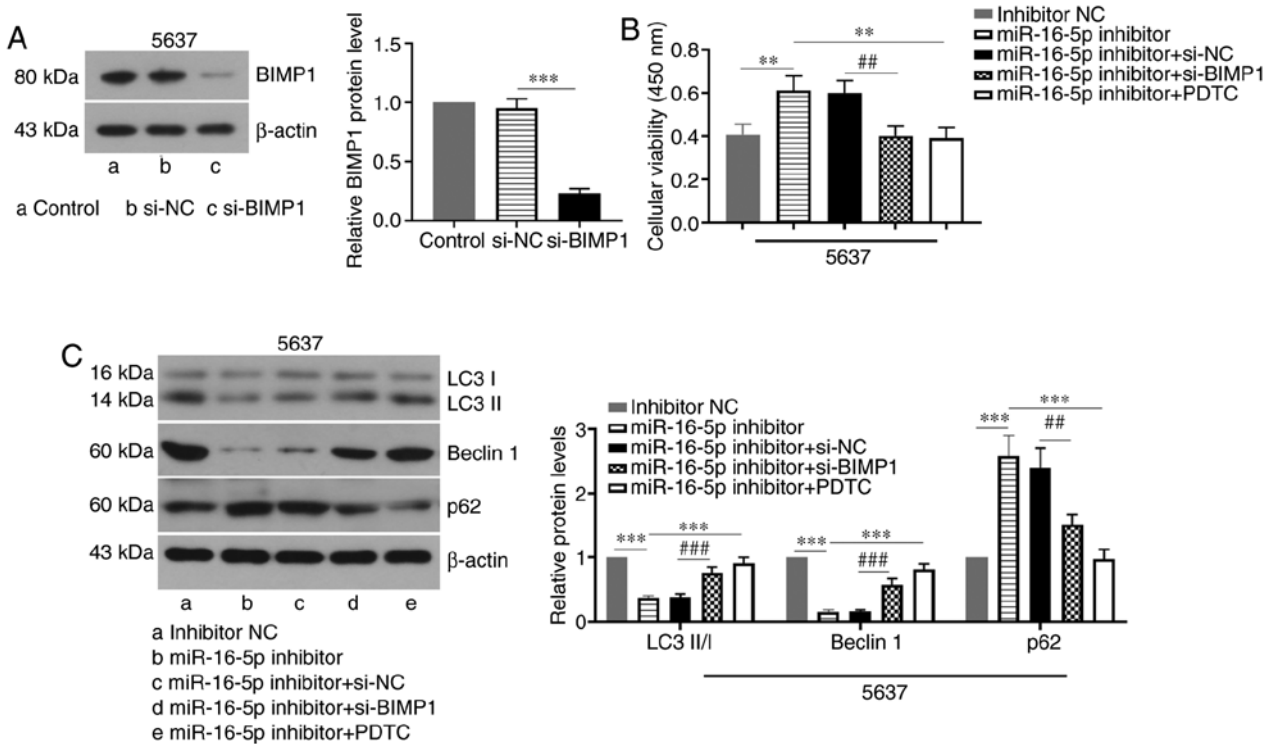
Figure 4. miR-16-5p promotes autophagy by blocking the BIMP1/NF-κB signaling pathway in bladder cancer cells. (A) The protein level of BIMP1 in 5637 cells transfected with si-BIMP1 or si-NC was evaluated by western blotting. (B and C) Viability and protein expression levels of LC3-II/I, beclin 1 and p62 in 5637 cells. The 5637 cells were co-transfected with miR-16-5p inhibitor and BIMP1 siRNA or its NC, or cells were transfected with miR-16-5p inhibitor followed by treatment with 20 μM PDTC (n=3). Data are presented as the means ± SD. **P<0.01, ***P<0.001, ##P<0.01, ###P<0.001. miR, microRNA; NC, negative control; PDTC, pyrrolidine dithiocarbamate; siRNA, small interfering RNA; LC3, microtubule-associated proteins 1A/1B light chain 3B; BIMP1, caspase recruitment domain family member 10.

organelles, autophagy reduces oxidative stress and oncogenic signaling, thereby inhibiting cancer progression (25). Although the role of autophagy in inhibiting human cancer is unclear, previous findings have suggested a role for autophagy stimulation in cancer prevention and treatment (26). The present study demonstrated that miR-16-5p induced autophagy in BC cells, as evidenced by increased autophagic flux, LC3-II/I ratio and beclin 1 protein expression, and decreased p62 expression in miR-16-5p-overexpressing BC cells. In addition, increasing evidence has demonstrated that there is crosstalk between autophagy and apoptosis during cancer development. Specifically, it has been reported that apoptotic inhibitors had no significant effect on autophagy in colorectal cancer cells, whereas 3-MA treatment or silencing autophagy-related gene 5 inhibits apoptosis in colorectal cancer cells (27). In addition, 3-MA administration reduces troglitazone-induced apoptosis in BC cells (28). The present results demonstrated that 3-MA treatment decreased miR-16-5p overexpression-induced apoptosis. These findings demonstrated that autophagy may act as an upstream mediator of apoptosis and activate apoptosis during the development of BC. Furthermore, it has been reported that beclin 1 is an important mediator of autophagy and apoptosis. Specifically, beclin 1 contains a Bcl-2 homology (BH)3 region, which physically interacts with Bcl-2/Bcl-xL proteins (29). BH3 domains bind to BH3 receptors and inhibit the anti-apoptotic Bcl-2 proteins, including Bcl-2, or activate the pro-apoptotic Bcl-2 family members, such as Bax (30). Thus, treatment with the autophagy inhibitor 3-MA may inhibit the apoptosis of BC cells by suppressing beclin 1.

BIMP1 is a scaffold protein that plays an important role in the development of cancer. It has been reported that BIMP1 is highly expressed in several types of cancer, including breast cancer, BC and colorectal cancer (31-33). Functional studies have revealed that BIMP1 is associated with cancer cell proliferation, migration, invasion and apoptosis, but whether BIMP1 regulates autophagy in BC cells remains largely unknown (14,32). BIMP1 has been reported to be associated with the NF-κB signaling pathway, and BIMP1 overexpression promotes breast cancer cell proliferation and suppresses apoptosis by activating the NF-κB signaling pathway (31). In addition, our previous study revealed that BIMP1 knockdown inhibited NF-κB signaling in BC cells (34).

The NF-κB signaling pathway is considered to be a positive regulatory pathway in cancer development (35). During cancer progression, the activation of the IκB protein by the IκB kinase complex leads to phosphorylation-induced proteasomal degradation of the IκB protein. The dimer (p50/p65) then forms and enters the nucleus to bind to the κB site in the target gene promoter or enhancer and further regulates gene expression (36). The NF-κB signaling pathway is a negative regulator of autophagy in several types of cancer. For example, baicalein induces autophagy in breast cancer cells by inhibiting the NF-κB signaling pathway (37). Dihydroartemisinin stimulates the induction of autophagy in human multiple myeloma, colorectal and cervical cancer cell lines via repression of the NF-κB signaling pathway (19). Taken together, these findings indicate that the BIMP1/NF-κB signaling pathway suppresses autophagy.
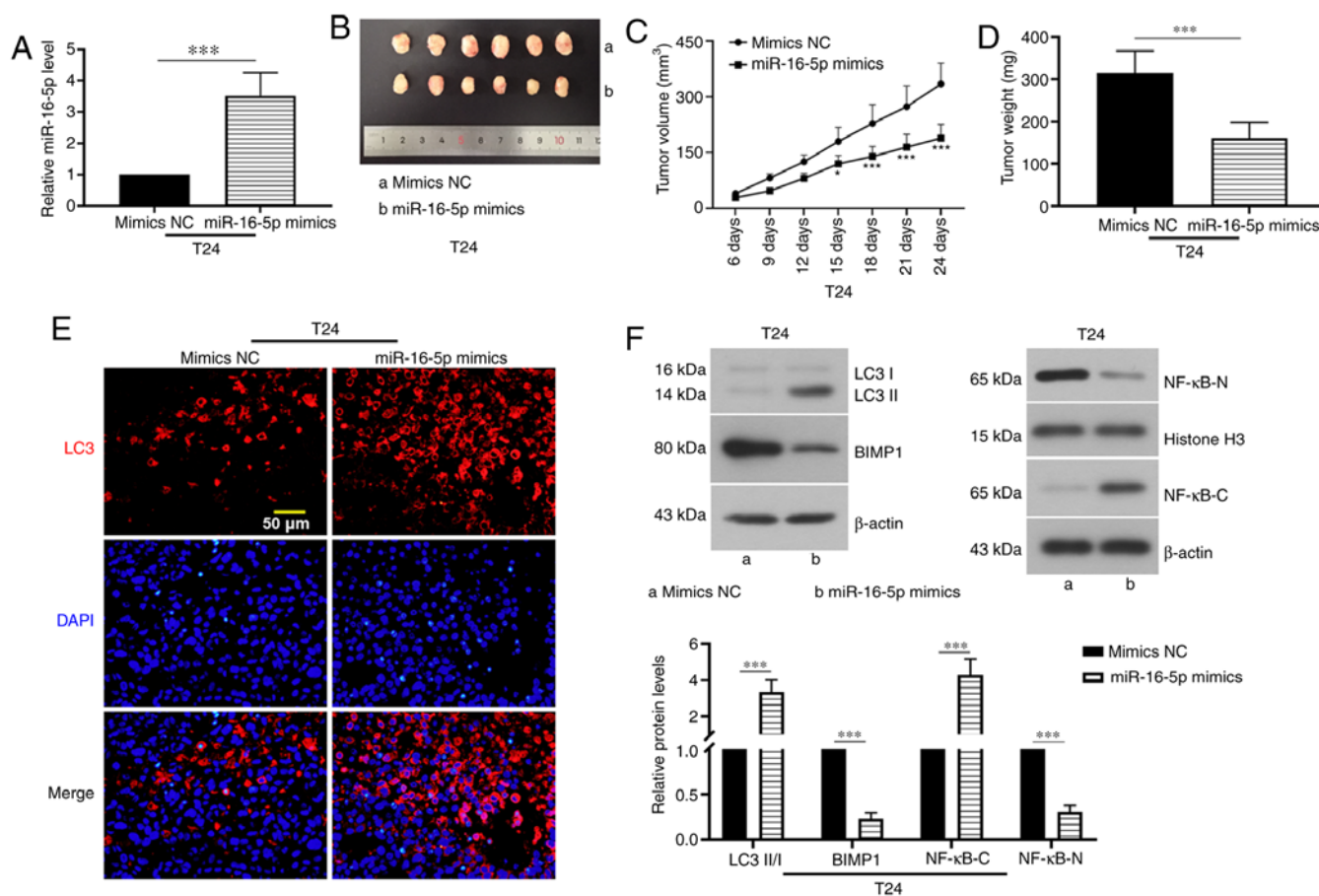
Figure 5. miR-16-5p overexpression suppresses tumor growth in mice. (A) The expression of miR-16-5p in tumor tissue samples was detected by reverse transcription-quantitative PCR after the mice were injected with T24 cells transfected with mimics NC or miR-16-5p mimics. (B) Macroscopic images of the tumors. (C) Tumor volume was measured every 3 days from day 6 onwards. (D) On day 24, tumor weight was recorded. (E) LC3 expression in tumor tissue samples was analyzed by immunofluorescence staining (magnification, x400). (F) The LC3-II/I ratio, BIMP1 protein expression and the nucleus (NF-κB-N)/cytoplasm (NF-κB-C) ratio of p65 in tumor tissue samples were detected by western blotting (n=6). Data are presented as the means ± SD. *P<0.05, ***P<0.001. miR, microRNA; NC, negative control; LC3, microtubule-associated proteins 1A/1B light chain 3B; BIMP1, caspase recruitment domain family member 10.

Additionally, the present study demonstrated that miR-16-5p directly targeted BIMP1 and suppressed its expression, suggesting that miR-16-5p is able to block the BIMP1/NF-κB signaling pathway by targeting BIMP1. It was demonstrated that BIMP1 inhibition or the blockade of the NF-κB signaling pathway restored the effects of miR-16-5p knockdown on cell autophagy, indicating that miR-16-5p induces autophagy in BC cells through blocking the BIMP1/NF-κB signaling pathway. However, a single miRNA can target multiple downstream genes. For example, AKT3 has been demonstrated to be a target gene of miR-16-5p (38), while AKT3 knockdown in glioblastoma multiforme cells induces autophagy w9). Therefore, miR-16-5p may also induce autophagy in BC cells by targeting AKT3, indicating that miR-16-5p may participate in the regulation of BC cell autophagy through various pathways, and the miR-16-5p/BIMP1/NF-κB axis may be one of multiple potential pathways. Collectively, these findings provide initial evidence that the miR-16-5p/BIMP1/NF-κB axis may serve as a potential therapeutic target for BC.

Acknowledgements

Not applicable.

Availability of data and materials

The datasets used and/or analyzed during the current study are available from the corresponding author on reasonable request.

Authors' contributions

JH and XM were involved in the study design and wrote the manuscript. ZQ, HZ and ZG performed the experiments. YJ, ZL and CK confirmed the authenticity of all the raw data and conducted the statistical analysis. All authors read and approved the final manuscript.

Ethics approval and consent to participate

The present study was approved by The China Medical University Laboratory Animal Welfare and Ethical Committee (approval no. KT2020037) and animal experiments were performed in accordance with the Guidelines for the Care and Use of Laboratory Animals.

Patient consent for publication

Not applicable.

Competing interests

The authors declare that they have no competing interests.

References

1. Antoni S, Ferlay J, Soerjomataram I, Znaor A, Jemal A and Bray F: Bladder cancer incidence and mortality: A global overview and recent trends. Eur Urol 71: 96-108, 2017.
2. Benhamou S, Bonastre J, Groussard K, Radvanyi F, Allory Y and Lebret T: A prospective multicenter study on bladder cancer: The COBLAnCE cohort. BMC Cancer 16: 837, 2016.
3. Racioppi M, D'Agostino D, Totaro A, Pinto F, Sacco E, D'Addessi A, Marangi F, Palermo G and Bassi PF: Value of current chemotherapy and surgery in advanced and metastatic bladder cancer. Urol Int 88: 249-258, 2012.
4. Blick C, Ramachandran A, McCormick R, Wigfield S, Cranston D, Catto J and Harris AL: Identification of a hypoxia-regulated miRNA signature in bladder cancer and a role for miR-145 in hypoxia-dependent apoptosis. Br J Cancer 113: 634-644, 2015.
5. van Rhijn BW, Burger M, Lotan Y, Solsona E, Stief CG, Sylvester RJ, Witjes JA and Zlotta AR: Recurrence and progression of disease in non-muscle-invasive bladder cancer: From epidemiology to treatment strategy. Eur Urol 56: 430-442, 2009.
6. Mizushima N and Komatsu M: Autophagy: Renovation of cells and tissues. Cell 147: 728-741, 2011.
7. Cheng Y, Li Z, Xie J, Wang P, Zhu J, Li Y and Wang Y: MiRNA-224-5p inhibits autophagy in breast cancer cells via targeting Smad4. Biochem Biophys Res Commun 506: 793-798, 2018.
8. Bartel DP: MicroRNAs: Target recognition and regulatory functions. Cell 136: 215-233, 2009.
9. Vishnoi A and Rani S: MiRNA biogenesis and regulation of diseases: An overview. Methods Mol Biol 1509: 1-10, 2017.
10. Huang N, Wu J, Qiu W, Lyu Q, He J, Xie W, Xu N and Zhang Y: MiR-15a and miR-16 induce autophagy and enhance chemosensitivity of camptothecin. Cancer Biol Ther 16: 941-948, 2015.
11. Jiang QQ, Liu B and Yuan T: MicroRNA-16 inhibits bladder cancer proliferation by targeting Cyclin D1. Asian Pac J Cancer Prev 14: 4127-4130, 2013.
12. Wang H, Zhang Y, Wu Q, Wang YB and Wang W: miR-16 mimics inhibit TGF-β1-induced epithelial-to-mesenchymal transition via activation of autophagy in non-small cell lung carcinoma cells. Oncol Rep 39: 247-254, 2018.
13. Xia ZX, Li ZX, Zhang M, Sun LM, Zhang QF and Qiu XS: CARMA3 regulates the invasion, migration, and apoptosis of non-small cell lung cancer cells by activating NF-κB and suppressing the P38 MAPK signaling pathway. Exp Mol Pathol 100: 353-360, 2016.
14. Zhang S, Zhang C, Liu W, Zheng W, Zhang Y, Wang S, Huang D, Liu X and Bai Z: MicroRNA-24 upregulation inhibits proliferation, metastasis and induces apoptosis in bladder cancer cells by targeting CARMA3. Int J Oncol 47: 1351-1360, 2015.
15. Patel M, Horgan PG, McMillan DC and Edwards J: NF-κB pathways in the development and progression of colorectal cancer. Transl Res 197: 43-56, 2018.
16. Zhang J, Kuang Y, Wang Y, Xu Q and Ren Q: Notch-4 silencing inhibits prostate cancer growth and EMT via the NF-κB pathway. Apoptosis 22: 877-884, 2017.
17. Wang C, Li A, Yang S, Qiao R, Zhu X and Zhang J: CXCL5 promotes mitomycin C resistance in non-muscle invasive bladder cancer by activating EMT and NF-κB pathway. Biochem Biophys Res Commun 498: 862-868, 2018.
18. Xiao G: Autophagy and NF-kappaB: Fight for fate. Cytokine Growth Factor Rev 18: 233-243, 2007.
19. Hu W, Chen SS, Zhang JL, Lou XE and Zhou HJ: Dihydroartemisinin induces autophagy by suppressing NF-κB activation. Cancer Lett 343: 239-248, 2014.
20. He HJ, Bing H and Liu G: TSR2 Induces laryngeal cancer cell apoptosis through inhibiting NF-κB signaling pathway. Laryngoscope 128: E130-E134, 2018.
21. Livak KJ and Schmittgen TD: Analysis of relative gene expression data using real-time quantitative PCR and the 2(-Delta Delta C(T)) method. Methods 25: 402-408, 2001.
22. National Research Council: Committee for the Update of the Guide for the Care and Use of Laboratory Animals. In: Guide for the Care and Use of Laboratory Animals. 8th edition. National Academies Press, Washington, DC, 2011.
23. Wang F, Wu H, Fan M, Yu R, Zhang Y, Liu J, Zhou X, Cai Y, Huang S, Hu Z and Jin X: Sodium butyrate inhibits migration and induces AMPK-mTOR pathway-dependent autophagy and ROS-mediated apoptosis via the miR-139-5p/Bmi-1 axis in human bladder cancer cells. FASEB J 34: 4266-4282, 2020.
24. Liu X, Li S, Li Y, Cheng B, Tan B and Wang G: Puerarin inhibits proliferation and induces apoptosis by upregulation of miR-16 in bladder cancer cell line T24. Oncol Res 26: 1227-1234, 2018.
25. White E, Mehnert JM and Chan CS: Autophagy, metabolism, and cancer. Clin Cancer Res 21: 5037-5046, 2015.
26. Levy JMM, Towers CG and Thorburn A: Targeting autophagy in cancer. Nat Rev Cancer 17: 528-542, 2017.
27. Won SJ, Yen CH, Liu HS, Wu SY, Lan SH, Jiang-Shieh YF, Lin CN and Su CL: Justicidin A-induced autophagy flux enhances apoptosis of human colorectal cancer cells via class III PI3K and Atg5 pathway. J Cell Physiol 230: 930-946, 2015.
28. Yan S, Yang X, Chen T, Xi Z and Jiang X: The PPARγ agonist Troglitazone induces autophagy, apoptosis and necroptosis in bladder cancer cells. Cancer Gene Ther 21: 188-193, 2014.
29. Maiuri MC, Le Toumelin G, Criollo A, Rain JC, Gautier F, Juin P, Tasdemir E, Pierron G, Troulinaki K, Tavernarakis N, *et al*: Functional and physical interaction between Bcl-X(L) and a BH3-like domain in Beclin-1. EMBO J 26: 2527-2539, 2007.
30. Galonek HL and Hardwick JM: Upgrading the BCL-2 network. Nat Cell Biol 8: 1317-1319, 2006.
31. Zhao T, Miao Z, Wang Z, Xu Y, Wu J, Liu X, You Y and Li J: CARMA3 overexpression accelerates cell proliferation and inhibits paclitaxel-induced apoptosis through NF-κB regulation in breast cancer cells. Tumour Biol 34: 3041-3047, 2013.
32. Man X, Liu T, Jiang Y, Zhang Z, Zhu Y, Li Z, Kong C and He J: Silencing of CARMA3 inhibits bladder cancer cell migration and invasion via deactivating β-catenin signaling pathway. Onco Targets Ther 12: 6309-6322, 2019.
33. Wang L, Qian L, Li X and Yan J: MicroRNA-195 inhibits colorectal cancer cell proliferation, colony-formation and invasion through targeting CARMA3. Mol Med Rep 10: 473-478, 2014.
34. Man X, He J, Kong C, Zhu Y and Zhang Z: Clinical significance and biological roles of CARMA3 in human bladder carcinoma. Tumour Biol 35: 4131-4136, 2014.
35. Xia Y, Shen S and Verma IM: NF-κB, an active player in human cancers. Cancer Immunol Res 2: 823-830, 2014.
36. Naugler WE and Karin M: NF-kappaB and cancer-identifying targets and mechanisms. Curr Opin Genet Dev 18: 19-26, 2008.
37. Yan W, Ma X, Zhao X and Zhang S: Baicalein induces apoptosis and autophagy of breast cancer cells via inhibiting PI3K/AKT pathway in vivo and vitro. Drug Des Devel Ther 12: 3961-3972, 2018.
38. Ruan L and Qian X: MiR-16-5p inhibits breast cancer by reducing AKT3 to restrain NF-κB pathway. Biosci Rep: Aug 23, 2019 (Epub ahead of print). doi: 10.1042/BSR20191611.
39. Paul-Samojedny M, Pudelko A, Kowalczyk M, Fila-Daniłow A, Suchanek-Raif R, Borkowska P and Kowalski J: Knockdown of AKT3 and PI3KCA by RNA interference changes the expression of the genes that are related to apoptosis and autophagy in T98G glioblastoma multiforme cells. Pharmacol Rep 67: 1115-1123, 2015.